Needle-Tissue Interaction Force Estimation using Residuals and Interaction Models

Medical Robotics Project

Gianmarco Roggiolani, Francesco Roscia, Matteo Sodano

January 2020

Goals

- Reconstruct the contact forces exerted on the needle mounted on the end-effector of a robot manipulator, in a sensorless fashion. The contact is seen as a fault in the actuation system

- Estimate needle-tissue interaction force and visco-elastic parameters of the tissue, and predict layer transition

Table of Contents

Table of Contents

Euler-Lagrange Model of a Manipulator

Dynamics of robot manipulator interacting at the contact point $\boldsymbol{x}_c \in \mathbb{R}^6$

$$\boldsymbol{B}(\boldsymbol{q})\ \ddot{\boldsymbol{q}} + \boldsymbol{C}(\boldsymbol{q}, \dot{\boldsymbol{q}})\ \dot{\boldsymbol{q}} + \boldsymbol{g}(\boldsymbol{q}) = \boldsymbol{\tau} + \boldsymbol{J}_c^T(\boldsymbol{q})\ \boldsymbol{F} = \boldsymbol{\tau}_{tot}$$

with

$\boldsymbol{q}, \dot{\boldsymbol{q}}, \ddot{\boldsymbol{q}}$	n	joint positions, velocities and accelerations
n	1	dimension of the configuration space
$\boldsymbol{B}$	$n \times n$	inertia matrix
$\boldsymbol{C}\,\dot{\boldsymbol{q}}$	n	centrifugal and Coriolis term
$\boldsymbol{g}$	n	gravity term
$\boldsymbol{\tau}$	n	control torque
$\boldsymbol{J}_c$	$6 \times n$	geometric Jacobian at $\boldsymbol{x}_c$
$\boldsymbol{F}$	6	force and moment exerted by the environment
$\boldsymbol{\tau}_{tot}$	n	total torque applied to the robot joints

The nonconservative forces are not modeled

Residual Method

Joint torque caused by the contact: $\boldsymbol{\tau}_c = \boldsymbol{J}_c^T(\boldsymbol{q})\,\boldsymbol{F}$

Generalized momentum

$$\boldsymbol{p} = \boldsymbol{B}(\boldsymbol{q})\ \dot{\boldsymbol{q}}$$

and its dynamics

$$\dot{\boldsymbol{p}} = \boldsymbol{\tau} + \boldsymbol{\tau}_c + \boldsymbol{C}^T(\boldsymbol{q}, \dot{\boldsymbol{q}})\ \dot{\boldsymbol{q}} - \boldsymbol{g}(\boldsymbol{q})$$

Decoupled dynamics: the i-th component of $\dot{\boldsymbol{p}}$ depends only on the i-th component of $\boldsymbol{\tau}_c$

Residual Method

We want to estimate the interaction force $\boldsymbol{F}$ having only the proprioceptive measurements $\boldsymbol{q}$, $\dot{\boldsymbol{q}}$, $\boldsymbol{\tau}$

Residual vector

$$\boldsymbol{r}(t) = \boldsymbol{K}\left[\boldsymbol{p}(t) - \int_0^t \left(\boldsymbol{\tau} + \boldsymbol{C}^T(\boldsymbol{q}, \dot{\boldsymbol{q}})\ \dot{\boldsymbol{q}} - \boldsymbol{g}(\boldsymbol{q}) + \boldsymbol{r}\right) ds - \boldsymbol{p}(0)\right]$$

with $\boldsymbol{K} > 0$ diagonal

Residual Method

Linear, decoupled and exponentially stable system fed by the contact torque $\boldsymbol{\tau}_c$

time domain $\qquad \dot{\boldsymbol{r}} = -\boldsymbol{K}\ \boldsymbol{r} + \boldsymbol{K}\ \boldsymbol{\tau}_c, \quad \boldsymbol{r}(0) = 0$

Laplace domain $\quad \dfrac{r_i(s)}{\tau_{c,i}(s)} = \dfrac{K_i}{s + K_i}, \quad i = 1, \ldots, n$

During free motion: $\boldsymbol{r} \approx \mathbf{0}$
A collision occurs: $\boldsymbol{r}$ varies. For large values of K_i, the residual vector reproduces the contact torque $r_i \rightarrow \tau_{c,i}$ ($\boldsymbol{\varepsilon} = \boldsymbol{\tau}_c - \boldsymbol{r} \approx 0$)
Contact is lost: the residual vector returns to zero

Isolation property: if the residual vector has the first i components different from zero and the others $n - i$ equal to zero, then a collision has occurred at link i

Residual Method

The contact force $\boldsymbol{F}$ is reconstructed as

$$\hat{\boldsymbol{F}}_{RES} = \left[\boldsymbol{J}_c^T(\boldsymbol{q})\right]^{\#} \boldsymbol{r}$$

Assuming a perfectly rigid needle, the penetration occurs only along the end-effector z-axis

We denote with $\hat{f}_{RES}$ the third component of $\hat{\boldsymbol{F}}_{RES}$

Discretization of Residual Equation

Euler integration with sampling time Δt of residual vector

$$\boldsymbol{r}(t) = \boldsymbol{K}\left[\boldsymbol{p}(t) - \int_0^t \left(\boldsymbol{\tau} + \boldsymbol{C}^T(\boldsymbol{q}, \dot{\boldsymbol{q}})\ \dot{\boldsymbol{q}} - \boldsymbol{g}(\boldsymbol{q}) + \boldsymbol{r}\right) ds - \boldsymbol{p}(0)\right]$$

as

$$\begin{aligned}
\boldsymbol{r}_k &= \boldsymbol{K}\left[\boldsymbol{B}_k\ \dot{\boldsymbol{q}}_k - \sum_{i=0}^{k}\left(\boldsymbol{\tau}_i + \boldsymbol{C}_i^T\ \dot{\boldsymbol{q}}_i - \boldsymbol{g}_i + \boldsymbol{r}_i\right)\ \Delta t - \boldsymbol{p}_0\right] \\
&= \boldsymbol{K}\left[\boldsymbol{B}_k\ \dot{\boldsymbol{q}}_k - \sum_{i=0}^{k}\left(\boldsymbol{\tau}_i + \boldsymbol{C}_i^T\ \dot{\boldsymbol{q}}_i - \boldsymbol{g}_i\right)\ \Delta t - \Big(\sum_{i=0}^{k-1}\boldsymbol{r}_i + \boldsymbol{r}_k\Big)\ \Delta t - \boldsymbol{p}_0\right]
\end{aligned}$$

Discretization of Residual Equation

Collecting $\boldsymbol{r}_k$

$$\left(\boldsymbol{I}_n + \boldsymbol{K}\ \Delta t\right)\boldsymbol{r}_k = \boldsymbol{K}\left[\boldsymbol{B}_k\ \dot{\boldsymbol{q}}_k - \sum_{i=0}^{k}\left(\boldsymbol{\tau}_i + \boldsymbol{C}_i^T\ \dot{\boldsymbol{q}}_i - \boldsymbol{g}_i\right)\ \Delta t - \sum_{i=0}^{k-1}\boldsymbol{r}_i\ \Delta t - \boldsymbol{p}_0\right]$$

Iterative expression of the residual:

$$\boldsymbol{r}_k = \left(\boldsymbol{I}_n + \boldsymbol{K}\ \Delta t\right)^{-1}\ \boldsymbol{K}\left[\boldsymbol{B}_k\ \dot{\boldsymbol{q}}_k - \sum_{i=0}^{k}\left(\boldsymbol{\tau}_i + \boldsymbol{C}_i^T\ \dot{\boldsymbol{q}}_i - \boldsymbol{g}_i\right)\ \Delta t - \sum_{i=0}^{k-1}\boldsymbol{r}_i\ \Delta t - \boldsymbol{p}_0\right]$$

setting $\boldsymbol{r}_0 = 0$

$\boldsymbol{I}_n + \boldsymbol{K}\ \Delta t$ is invertible since $\boldsymbol{K} > 0$

Table of Contents

Needle Insertion Problem

1. No contact phase: the needle is approaching the tissue
2. Contact phase: the boundary of the tissue deflects, the needle is not penetrating the tissue
3. Puncture event: the tissue surface is breached
4. Tip and shaft insertion: a friction force due to the increasing contact area between the needle shaft and the tissue is experienced
5. Retraction: a friction force with opposite sign acts on the needle shaft

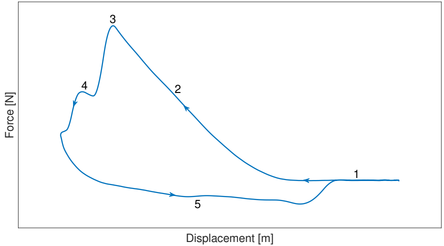

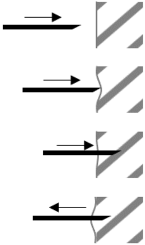

Interaction Model

$p(t)$: position of the tip of the needle with respect to the base frame.
Kelvin-Voigt model:

$$f(t) = -K(t)\,p(t) - B(t)\,\dot{p}(t)$$

where

- f: interaction force
- K: elastic coefficient (resistance of the layer surface to the needle insertion)
- B: damping coefficient (viscous friction along the needle)

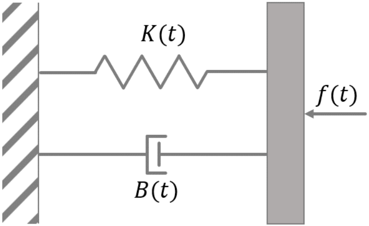

Interaction Model

Defining

$$\boldsymbol{\varphi}(t) = \begin{bmatrix} -p(t) & -\dot{p}(t) \end{bmatrix}^T$$
$$\boldsymbol{\theta}(t) = \begin{bmatrix} K(t) & B(t) \end{bmatrix}^T$$

the Kelvin-Voigt model can be rewritten as

$$\begin{aligned} f(t) &= -K(t)\,p(t) - B(t)\,\dot{p}(t) \\ &= \boldsymbol{\varphi}^T(t)\;\boldsymbol{\theta}(t) \end{aligned}$$

Interaction Force Prediction

A Recursive Least Square (RLS) algorithm is used to estimate $f(t)$

$\boldsymbol{\theta}_k$ and its covariance matrix $\boldsymbol{\Psi}_k$ are estimated as

$$\hat{\boldsymbol{\theta}}_k = \hat{\boldsymbol{\theta}}_{k-1} + \frac{\boldsymbol{\Psi}_{k-1} \ \boldsymbol{\varphi}_k \ e_k}{\lambda_k + \boldsymbol{\varphi}_k^T \ \boldsymbol{\Psi}_{k-1} \ \boldsymbol{\varphi}_k}$$

$$\boldsymbol{\Psi}_k = \boldsymbol{\Psi}_{k-1} - \frac{\boldsymbol{\Psi}_{k-1} \ \boldsymbol{\varphi}_k \ \boldsymbol{\varphi}_k^T \ \boldsymbol{\Psi}_{k-1}}{\lambda_k + \boldsymbol{\varphi}_k^T \ \boldsymbol{\Psi}_{k-1} \ \boldsymbol{\varphi}_k}$$

where $\lambda_k \in \big(0, 1\big]$ is the forgetting factor. We use $\lambda_k = 1, \forall k$

The estimated interaction force

$$\hat{f}_k = \boldsymbol{\varphi}_k^T \ \hat{\boldsymbol{\theta}}_{k-1}$$

Interaction Force Prediction

Covariance Resetting

$\exists\, k^* > 0 \,:\, \mathrm{tr}\left(\boldsymbol{\Psi}_{k^*}\right) < \mathrm{th} \Rightarrow \boldsymbol{\Psi}_{k^*} \leftarrow \boldsymbol{\Psi}_0$

This method is used for having an estimation algorithm more sensitive to parameters variations

Initialization

The initial value of the Kelvin-Voigt parameters $\hat{\boldsymbol{\theta}}_0$ is set as

$$\hat{\boldsymbol{\theta}}_0 = \left[\boldsymbol{\varphi}_0^T\right]^{\#} f_0$$

Layer Transitions

$\hat{f}_k$ should reconstruct well f_k unless an abrupt change happens: this is due to a layer rupture

Estimation Error	$e_k = f_k - \hat{f}_k$
Distance Function	$s_k = e_k^2$
Threshold	$\gamma = \dfrac{\sigma_1^2 - \sigma_0^2}{2}$
Drift	$\nu = \dfrac{\sigma_1^2 + \sigma_0^2}{2}$

where σ_0^2 and σ_1^2 are the variances of the error function in the default and abrupt change case

Layer Transitions

We define the Decision Function as

$$g_k = \max\{g_{k-1} + s_k - \nu, 0\}$$

When $g_k > \gamma$, a puncturing event is supposed to occur

$$\mathrm{Flag}\ (g_k) = \begin{cases} 1, \ \text{if } g_k > \gamma \\ 0, \ \text{otherwise} \end{cases}$$

A layer transition is expected when Flag raises

Layer Transitions

An off-line method for identifying σ_0 and σ_1 based on a statistical analysis of e_k and $\dot{e}_k$ is introduced

1. From f, identify the number N of expected layer transitions. Each transition introduces a peak in e (i.e., two consecutive peaks in $\dot{e}$)

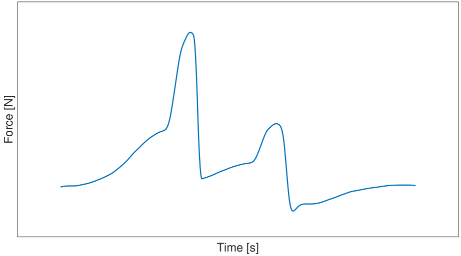

Layer Transitions

2. Sort the local maxima of $|\dot{e}|$ in decreasing order. Call ρ the value of the $(2N+1)-th$ one: it should not depend on any abrupt event

3. Consider the $i-th$ abrupt event and its pair of peaks in $\dot{e}$. Call:
   - $t_{\mathrm{IN},i}$ the first time instant for which $\dot{e}(t_{\mathrm{IN},i}) \leq -\rho$
   - $t_{\mathrm{FIN},i}$ the last time instant for which $\dot{e}(t_{\mathrm{FIN},i}) \geq \rho$

$\Omega = \bigcup_i \, [t_{\mathrm{IN},i}, t_{\mathrm{FIN},i}]$: set of times for which a puncture is expected

$\Xi = \bigcup_i \, [t_{\mathrm{FIN},i}, t_{\mathrm{IN},i+1}]$: set of the other time instants

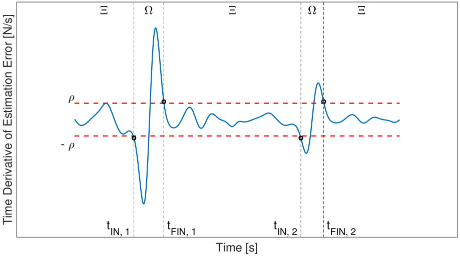

Layer Transitions

4. Compute σ_0 and σ_1 as

$$\sigma_0 = \mathrm{std}(e(t)), \quad t \in \Xi$$
$$\sigma_1 = \mathrm{std}(e(t)), \quad t \in \Omega$$

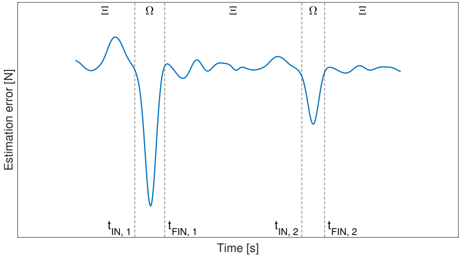

Table of Contents

Experimental Setup

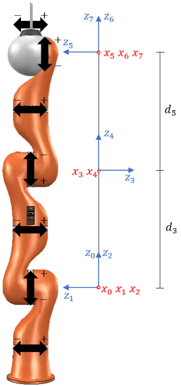

i	a	α	d	θ
1	0	$\pi/2$	0	q_1
2	0	$-\pi/2$	0	q_2
3	0	$-\pi/2$	0.40	q_3
4	0	$\pi/2$	0	q_4
5	0	$\pi/2$	0.39	q_5
6	0	$-\pi/2$	0	q_6
7	0	0	0	q_7

A force/torque sensor is mounted on the robot end-effector

Needle length: 0.23 m

Data have been filtered by means of a non-causal Butterworth filter

Experimental Setup

Experiments on gels (with different densities) and liver

- Sinusoidal automatic trajectory starting in contact
- Sinusoidal automatic trajectory starting not in contact
- Teleoperated trajectory driven by Geomagic Touch

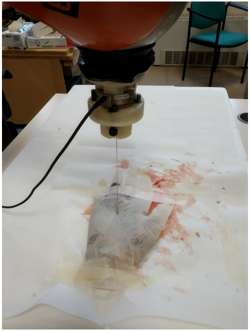

Experimental Setup

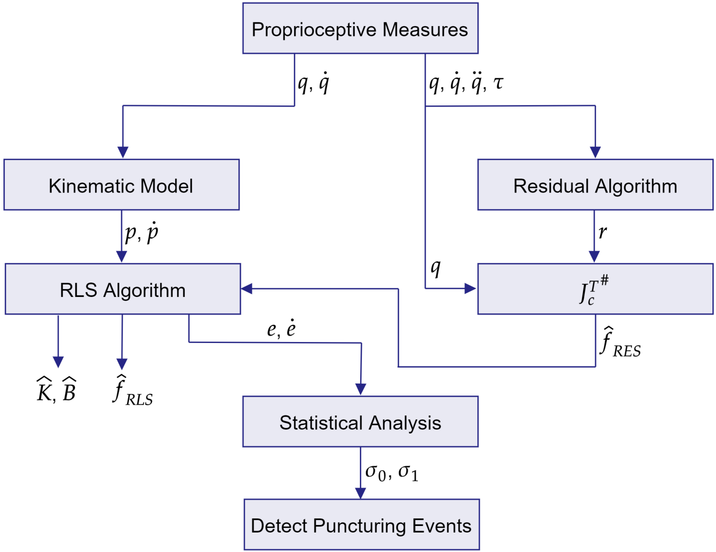

Table of Contents

Simulation 1

Sinusoidal Automatic Trajectory on Gel - Starting in Contact

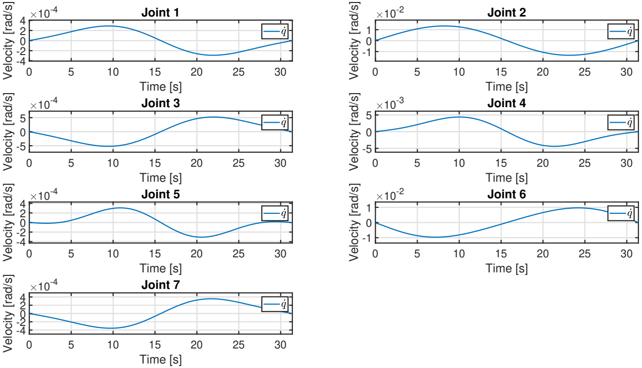

Figure: Joint velocities

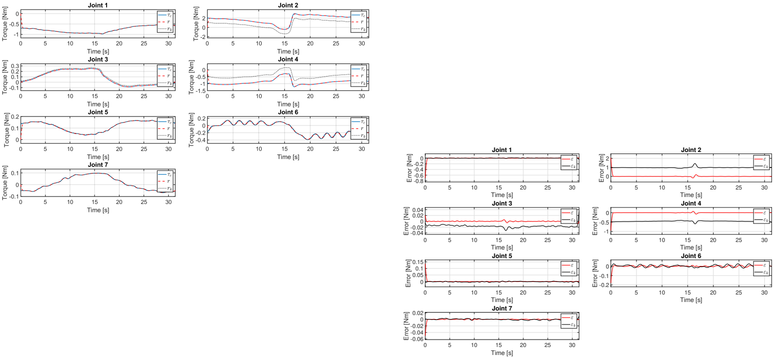

Figure: Left: Disturbance joint torque (blue), residuals (red) and residuals retrieved from the Fast Research Interface of KUKA (black). Right: Reconstruction error of residuals (red) and residuals retrieved from the Fast Research Interface of KUKA (black)

Simulation 1

Sinusoidal Automatic Trajectory on Gel - Starting in Contact

$\hat{f}_{RES}$ is expressed with respect to a frame attached on the needle tip
f is expressed with respect to a frame attached on the last joint
Then $\hat{f}_{RES}$ must be computed on the 7th frame for the comparison with f

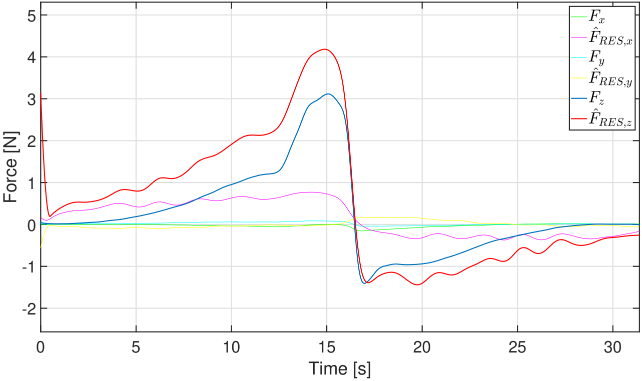

Figure: Measured force and reconstructed force from residuals

The second rupture is a false positive. Even if the needle is pushing on the underlying layer, the rupture does not occur

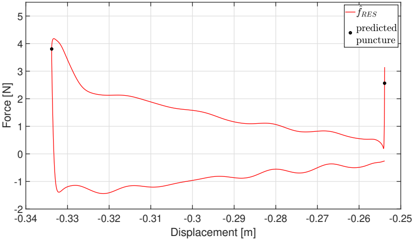

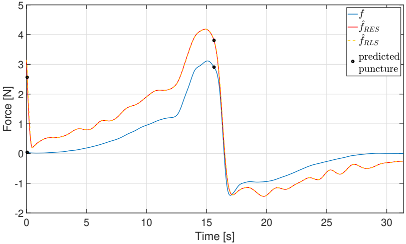

Figure: Evolution of the interaction force as a function of displacement (left) and time (right). The black points represent the predicted layer transitions

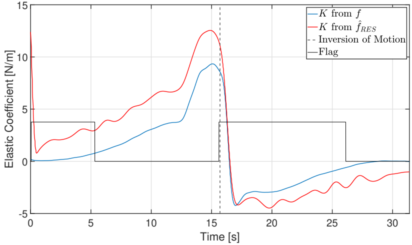

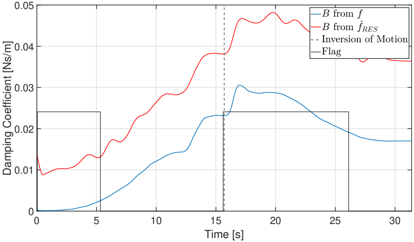

Figure: Predicted elastic (left) and damping (right) coefficients, with flag function. In blue, the coefficients obtained from the measured force; in red, the coefficients obtained from the residual force

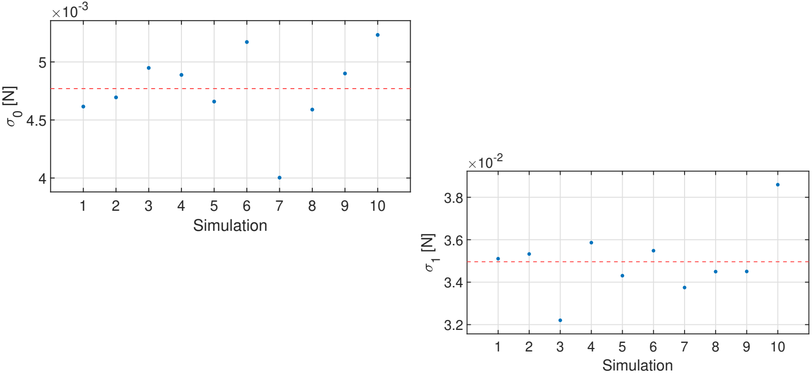

Figure: Values of σ_0 (a) and σ_1 (b) for each experiment and their average (red)

Simulation 2

Sinusoidal Automatic Trajectory on Gel - Starting not in Contact

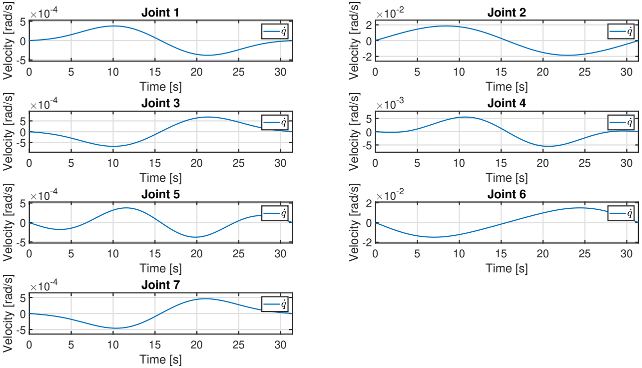

Figure: Joint velocities

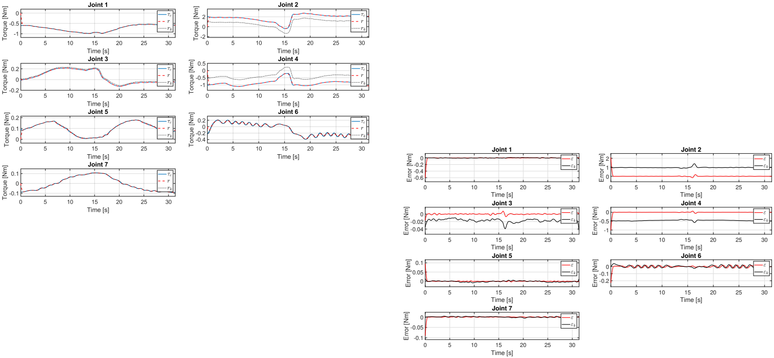

Figure: Left: Disturbance joint torque (blue), residuals (red) and residuals retrieved from the Fast Research Interface of KUKA (black). Right: Reconstruction error of residuals (red) and residuals retrieved from the Fast Research Interface of KUKA (black)

Simulation 2

Sinusoidal Automatic Trajectory on Gel - Starting not in Contact

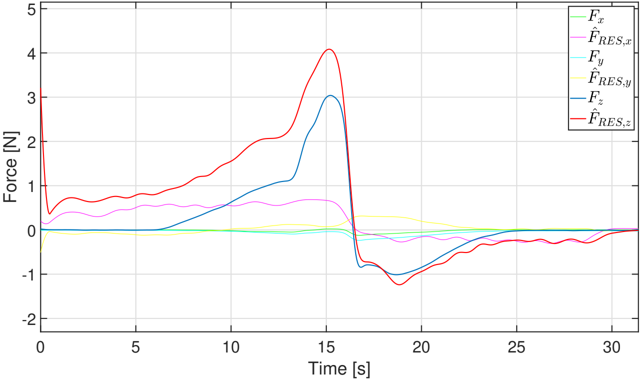

Figure: Measured force and reconstructed force from residuals

Simulation 2

Sinusoidal Automatic Trajectory on Gel - Starting not in Contact

The second rupture is a false positive. Even if the needle is pushing on the underlying layer, the rupture does not occur

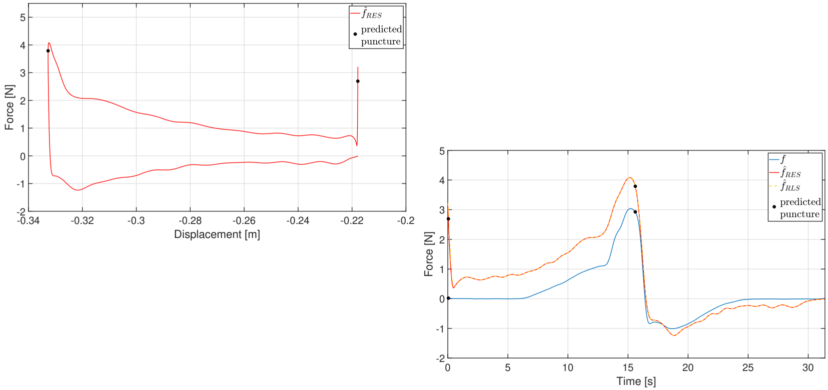

Figure: Evolution of the interaction force as a function of displacement (left) and time (right). The black points represent the predicted layer transitions

Sinusoidal Automatic Trajectory on Gel - Starting not in Contact

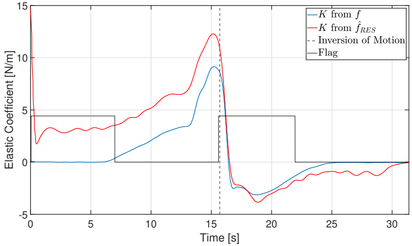

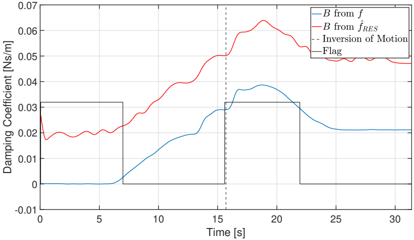

Figure: Predicted elastic (left) and damping (right) coefficients, with flag function. In blue, the coefficients obtained from the measured force; in red, the coefficients obtained from the residual force

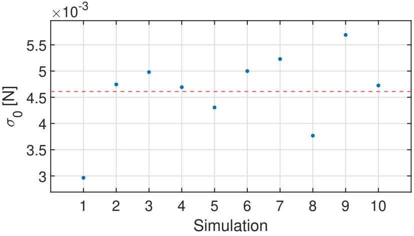

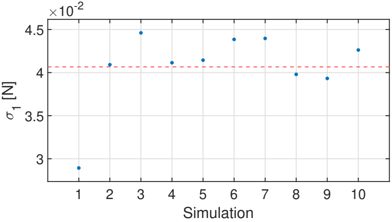

Figure: Values of σ_0 (a) and σ_1 (b) for each experiment and their average (red)

Simulation 3

Teleoperated Trajectory on Gel

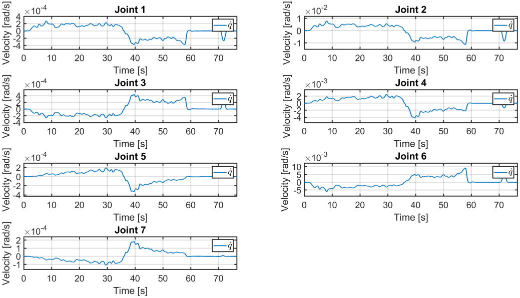

Figure: Joint velocities

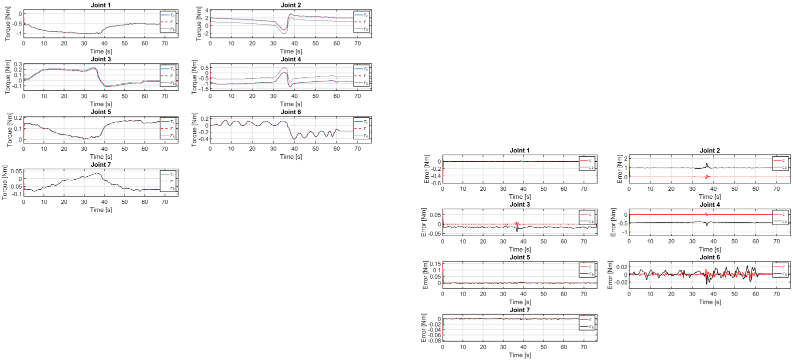

Figure: Left: Disturbance joint torque (blue), residuals (red) and residuals retrieved from the Fast Research Interface of KUKA (black). Right: Reconstruction error of residuals (red) and residuals retrieved from the Fast Research Interface of KUKA (black)

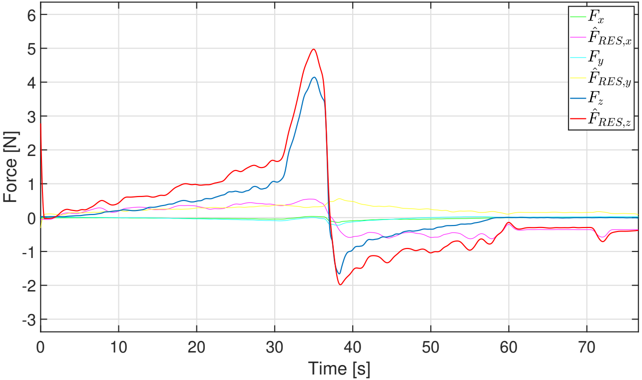

Figure: Measured force and reconstructed force from residuals

The second rupture is a false positive. Even if the needle is pushing on the underlying layer, the rupture does not occur

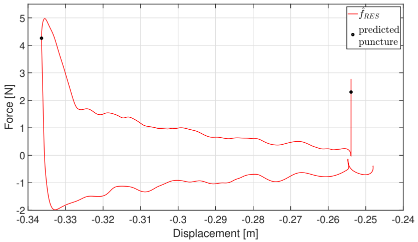

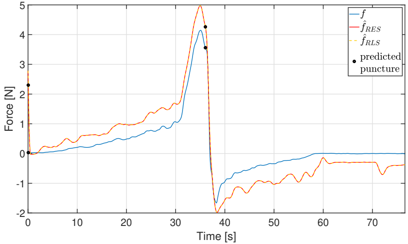

Figure: Evolution of the interaction force as a function of displacement (left) and time (right). The black points represent the predicted layer transitions

Simulation 3

Teleoperated Trajectory on Gel

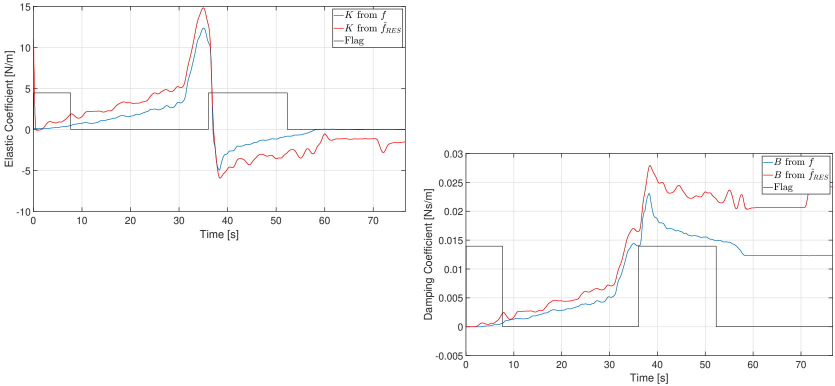

Figure: Predicted elastic (left) and damping (right) coefficients, with flag function. In blue, the coefficients obtained from the measured force; in red, the coefficients obtained from the residual force

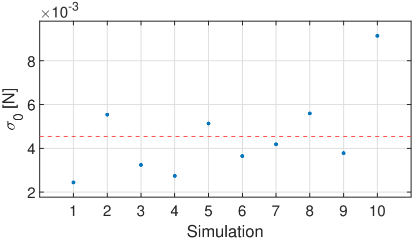

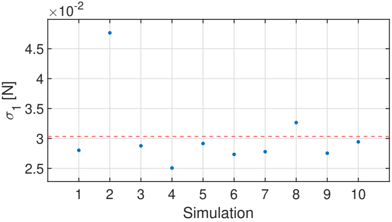

Figure: Values of σ_0 (a) and σ_1 (b) for each experiment and their average (red)

Simulation 4

Sinusoidal Automatic Trajectory on Liver

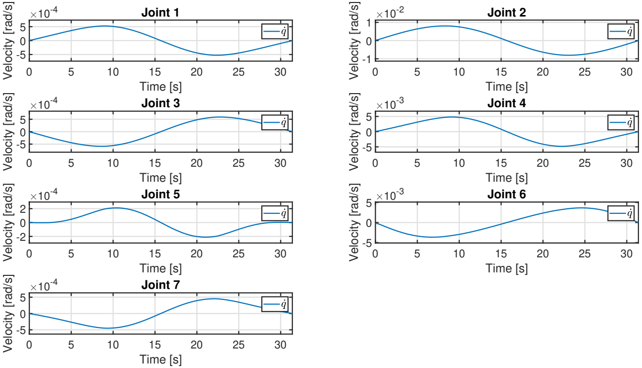

Figure: Joint velocities

Simulation 4

Sinusoidal Automatic Trajectory on Liver

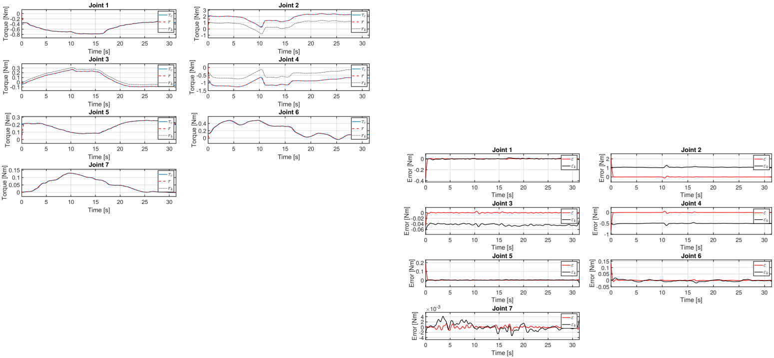

Figure: Left: Disturbance joint torque (blue), residuals (red) and residuals retrieved from the Fast Research Interface of KUKA (black). Right: Reconstruction error of residuals (red) and residuals retrieved from the Fast Research Interface of KUKA (black)

Simulation 4

Sinusoidal Automatic Trajectory on Liver

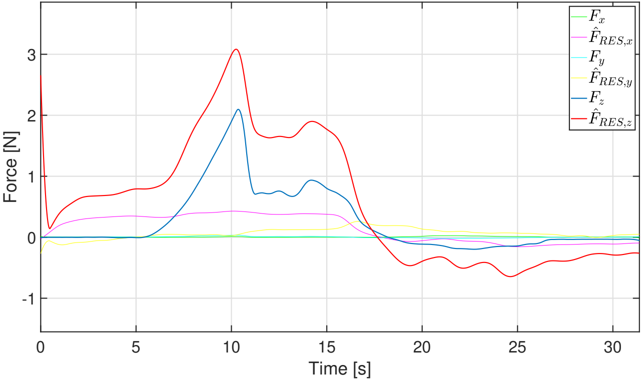

Figure: Measured force and reconstructed force from residuals

Simulation 4

Sinusoidal Automatic Trajectory on Liver

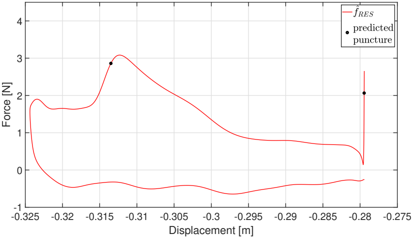

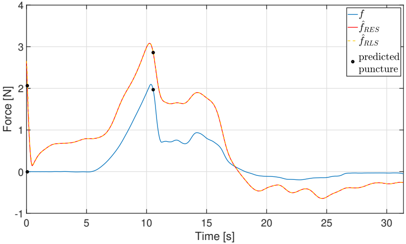

Figure: Evolution of the interaction force as a function of displacement (left) and time (right). The black points represent the predicted layer transitions

Simulation 4

Sinusoidal Automatic Trajectory on Liver

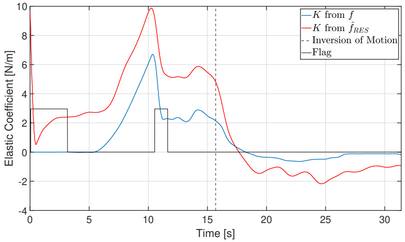

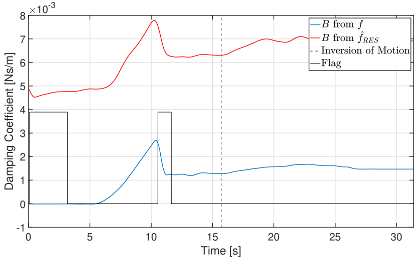

Figure: Predicted elastic (left) and damping (right) coefficients, with flag function. In blue, the coefficients obtained from the measured force; in red, the coefficients obtained from the residual force

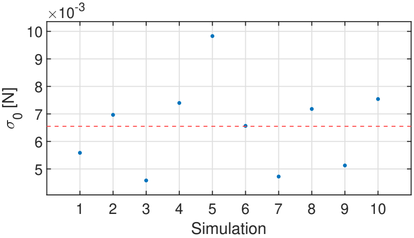

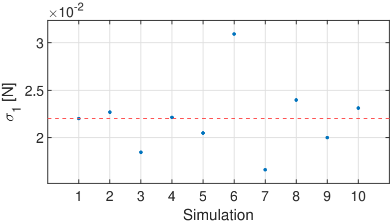

Figure: Values of σ_0 (a) and σ_1 (b) for each experiment and their average (red)

Simulation 4

Sinusoidal Automatic Trajectory on Liver – Model with Friction

This simulation is repeated considering also nonconservative forces

Friction torque $\boldsymbol{\tau}_f$ to be considered in the residual method:

$$\boldsymbol{\tau} \rightarrow \boldsymbol{\tau} - \boldsymbol{\tau}_f(\dot{\boldsymbol{q}})$$

New dynamical model:

$$\boldsymbol{B}(\boldsymbol{q})\ \ddot{\boldsymbol{q}} + \boldsymbol{C}(\boldsymbol{q}, \dot{\boldsymbol{q}})\ \dot{\boldsymbol{q}} + \boldsymbol{g}(\boldsymbol{q}) = \boldsymbol{\tau} - \boldsymbol{\tau}_f(\dot{\boldsymbol{q}}) + \boldsymbol{J}_c^T(\boldsymbol{q})\ \boldsymbol{F} = \boldsymbol{\tau}_{tot}$$

Results are comparable to the previous case

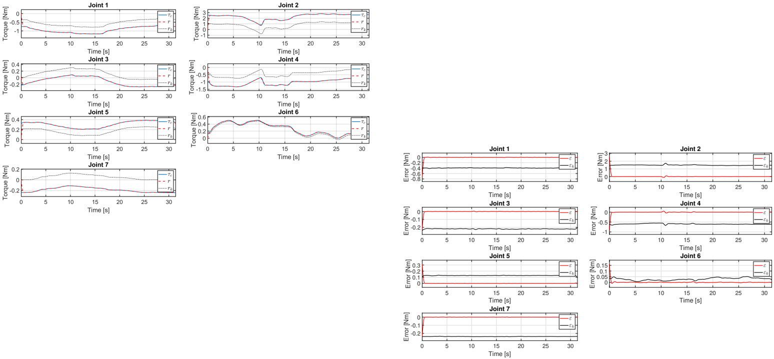

Figure: Left: Disturbance joint torque (blue), residuals obtained using the model with joint friction (red) and residuals retrieved from the FRI of KUKA (black). Right: Reconstruction error of residuals obtained using the model with joint friction (red) and residuals retrieved from the FRI of KUKA (black)

Simulation 4

Sinusoidal Automatic Trajectory on Liver – Model with Friction

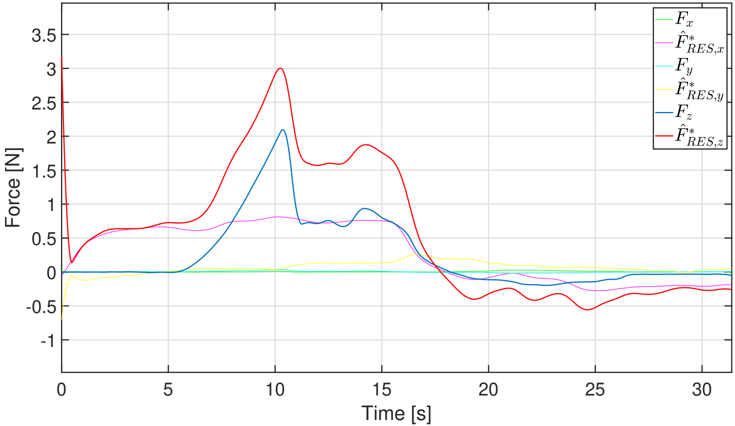

Figure: Measured force and reconstructed force from residuals obtained using the model with joint friction

Simulation 4

Sinusoidal Automatic Trajectory on Liver – Model with Friction

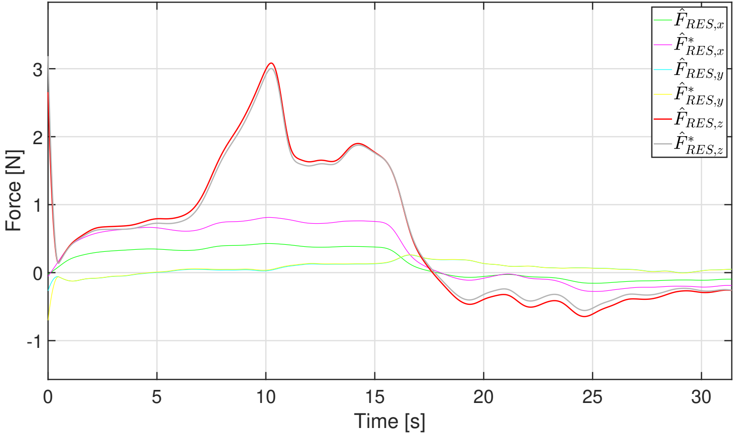

Figure: Components of the force reconstructed from residuals using the model without friction and the model with friction. The symbol * denotes variables retrieved by the model with joint friction

Simulation 4

Sinusoidal Automatic Trajectory on Liver – Model with Friction

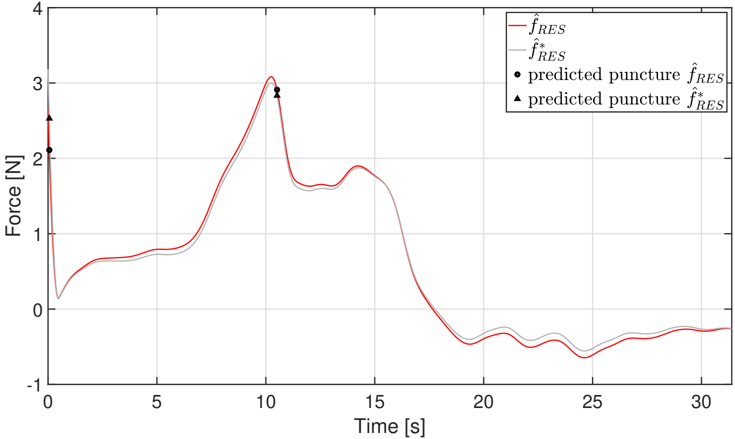

Figure: Evolution of the interaction force as a function of displacement. The black points represent the predicted layer transitions. The symbol * denotes variables retrieved by the model with joint friction

Simulation 4

Sinusoidal Automatic Trajectory on Liver – Model with Friction

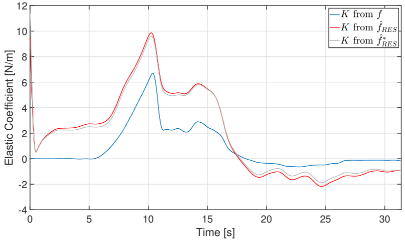

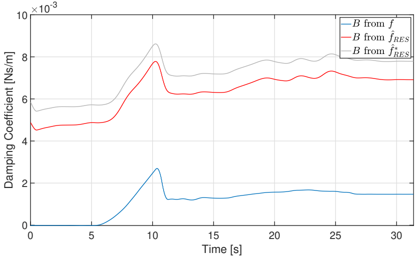

Figure: Predicted elastic (left) and damping (right) coefficients. In blue, the coefficients obtained from the measured force; in red, the coefficients obtained from the residual force using model without friction; in grey, the coefficients obtained from the residual force using model with friction. The symbol * denotes variables retrieved by the model with joint friction

Simulation 5

Teleoperated Trajectory on Liver

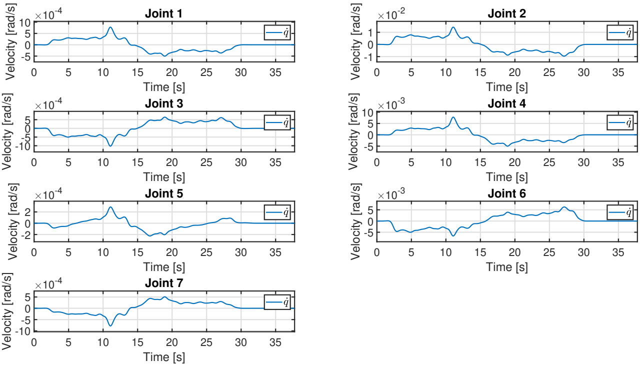

Figure: Joint velocities

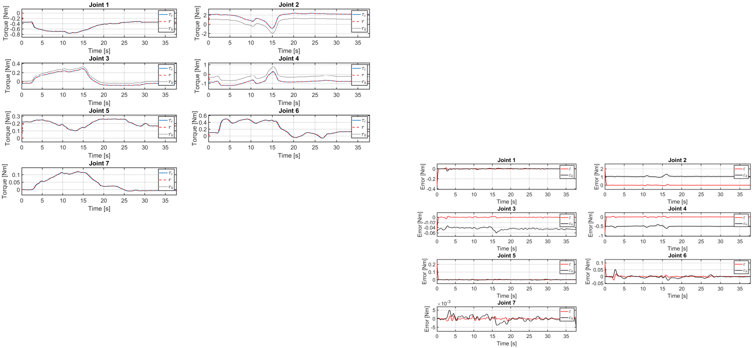

Figure: Left: Disturbance joint torque (blue), residuals (red) and residuals retrieved from the Fast Research Interface of KUKA (black). Right: Reconstruction error of residuals (red) and residuals retrieved from the Fast Research Interface of KUKA (black)

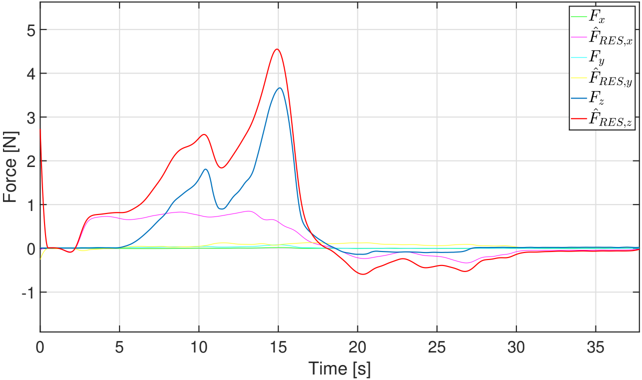

Figure: Measured force and reconstructed force from residuals

The second rupture is a false positive. Even if the needle is pushing on the underlying layer, the rupture does not occur

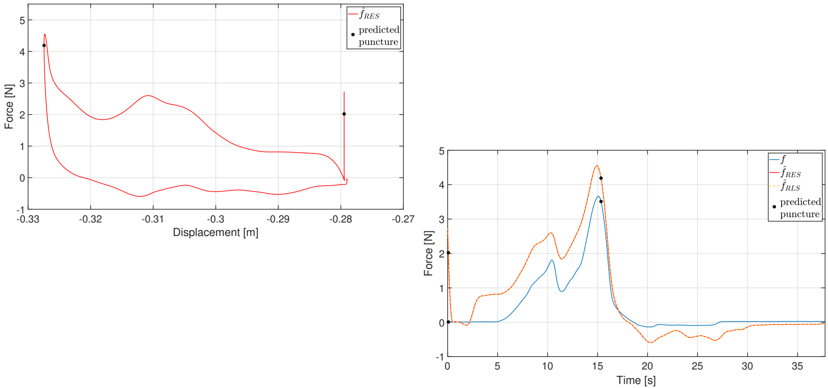

Figure: Evolution of the interaction force as a function of displacement (left) and time (right). The black points represent the predicted layer transitions

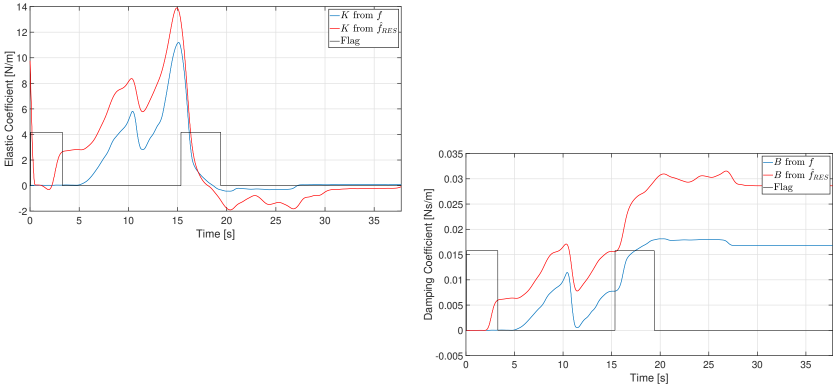

Figure: Predicted elastic (left) and damping (right) coefficients, with flag function. In blue, the coefficients obtained from the measured force; in red, the coefficients obtained from the residual force

Simulation 5

Teleoperated Trajectory on Liver

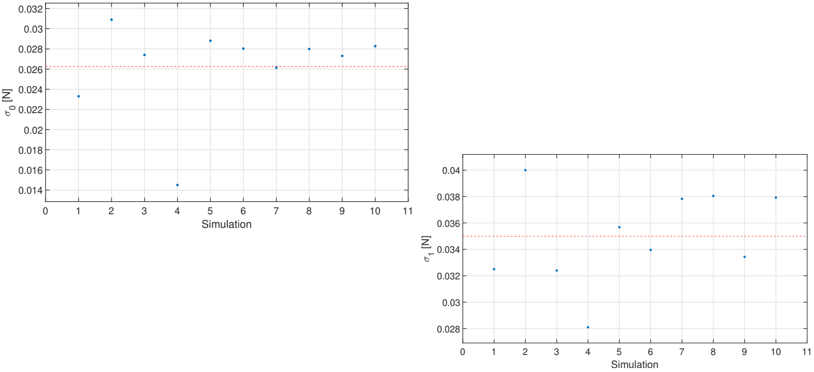

Figure: Values of σ_0 (a) and σ_1 (b) for each experiment and their average (red)

Table of Contents

Conclusions

The needle insertion problem has been addressed

- Contact of the needle with a tissue seen as a fault event
- Residual method for estimating the interaction force
- Recursive Least Squares algorithm for computing the visco-elastic parameters and for predicting rupture events
- Results on tissues of different nature

Thanks for your attention